A Two-Dimensional Model for Water Quality Simulation in lakes and its Aplication to Tabiishidani Lake in Sasaguri : Fukuoka Prefecture,Japan

Lap, Bui Quoc
Graduate School of Bioresource and Bioenvironmental Sciences, Kyushu Unviersity

Mori, Ken
Faculty of Agriculture, Kyushu Unviersity

https://doi.org/10.5109/4704

出版情報：九州大学大学院農学研究院紀要. 51 (1), pp.19-27, 2006-02-01. Faculty of Agriculture, Kyushu University
バージョン：
権利関係：

J. Fac. Agr., Kyushu Univ., **51** (1), 19–27 (2006)

A Two–Dimensional Model for Water Quality Simulation in lakes and its Application to Tabiishidani Lake in Sasaguri – Fukuoka Prefecture, Japan

Bui Quoc LAP[1] and Ken MORI*

Laboratory of Bioproduction and Environment Information Sciences, Division of Bioproduction and Environment Information Sciences, Department of Bioproduction and Environment Science, Faculty of Agriculture,Kyushu University, Fukuoka 812–8581, Japan
(Received October 24, 2005 and accepted November 16, 2005)

The objective of this research is to build a two–dimensional, unsteady, laterally averaged model for simulating water quality in lakes. The model consists of calculation of flow field and water quality simulation in lakes. The main foundation of the model is two–dimentional equations of the incompressible Navier–Stokes equations for circulation simulation and diffusion equations for water quality simulation. These equations were discretized by the finite volume method (FVM) and were solved for flow field velocities and water quality variables respectively by the SIMPLE (Semi–Implicit Method for Pressure–Linked Equations) algorithm (Patankar, 1980) with variables defined on a space–staggered rectangular grid. To solve these discretized equations effectively, a numerical method has been developed and coded in Fortran 90 (Nyhoff and Leestma, 1997; 1999) with using the Tri–Diagonal Matrix Algorithm (TDMA). To verify the model, Tabiishidani lake, which is located in Sasaguri–Fukuoka prefecture, Japan, was chosen as a case study. The Tabiishidani lake's water temperature, the size of cross–sections of the lake and meteorological data have been collected and used as the initial and boundary conditions for the model. After calibration, the model was applied to simulate water temperature in the Tabiishidani lake under different patterns of meteorology. Within this study, only water temperature was chosen to illustrate the methodology. However, this model can be extended to simulate any variable of water quality in lakes. The results of this research indicate that this model can be a useful tool for simulating water quality in lakes.

INTRODUCTION

Lakes and reservoirs are major surface water sources for life. They provide a multitude of uses including drinking, municipal water supply, power generation, navigation, agricultural irrigation, etc., and are prime regions for human settlement and habitation, but they may be also subject to pollution caused by these and other activities, which degrades their water quality further and further. Therefore, maintaining good water quality of lakes and reservoirs is great of significance, especially necessary for recent era where almost of water resources including surface and underground water are being threaten to degradation of both quantity and quality. To manage and maintain water quality in lakes and reservoirs, the alteration of their water quality parameters in response to external and internal sources must be understood. One effective way to gain insight into changes in their water quality is to apply numerical method to simulate the response to external and internal sources. In the growth of water quality modeling, in contrast to flowing waters, lakes and impoundments were not emphasized in the early years of water quality modeling because they have not historically been the major focus of urban development (Chapra, 1997). Therefore, compared with rivers and streams, a number of water quality models for lakes and impoundments are still limited. Some popular models for simulating water quality in lakes and reservoirs are DYRESM (Imberger and Patterson, 1981), CE–QUAL–W2 (Cole and Buchak, 1995). Our main concern with using the existing models is that they are not appropriate in some cases due to their complexity or to their need for an excessive number of inputs to the programs. Complex water quality models such as CE–QUAL–W2 require many types of data (Rounds and Wood, 2001). In an effort to contribute to the comprehensive understanding of water quality in lakes and reservoirs, this research has been done on the basis of mathematical discipline in order to develop a model for simulating their water quality. The model is established on the basis of the simplifying assumption that the flow in lakes is well–mixed laterally.

For simulation of water quality in lakes and reservoirs, how to calculate the flow field induced by wind as well as characterizing their process of circulation is necessary because the wind–induced flow significantly affects water quality in the closed–water area (Mori *et al.*, 2001). However, it is one of the key problems for the flow calculation because the flow field in lakes and reservoirs are very complex. To deal with this problem, the SIMPLE algorithm (Patankar, 1980) has been applied with the support of the Tri–Diagonal Matrix Algorithm (TDMA).

To verify the model, it is used to calibrate water temperature of the Tabiishidani lake against the observed data as a case study. After calibration, the model was applied to simulate water temperature in the lake under differ-

[1] Laboratory of Bioproduction and Environment Information Sciences, Division of Bioproduction and Environment Information Sciences, Department of Bioproduction and Bioenvironment Sciences, Graduate School of Bioresource and Bioenvironmental Sciences, Kyushu University

* Corresponding author (Email: moriken@bpes.kyushu–u.ac.jp)

ent patterns of meteorology in the lake area.

MATERIALS AND METHODS

Governing equations

The present numerical simulations are concerned with an unsteady-state, two-dimensional, laterally averaged flow, which is governed by a set of partial differential equations. The momentum and continuity equations in their primitive form are shown below :

$$\frac{\partial(\rho u)}{\partial x}+\frac{\partial(\rho w)}{\partial z}=0 \tag{1}$$

$$\frac{\partial(\rho u)}{\partial t}+\frac{\partial(\rho uu)}{\partial x}+\frac{\partial(\rho uw)}{\partial z}= -\frac{\partial p}{\partial x}+\frac{\partial}{\partial x}\left(\mu_x\frac{\partial u}{\partial x}\right)+\frac{\partial}{\partial z}\left(\mu_z\frac{\partial u}{\partial z}\right) \tag{2}$$

$$\frac{\partial(\rho w)}{\partial t}+\frac{\partial(\rho wu)}{\partial x}+\frac{\partial(\rho ww)}{\partial z}= -\rho g-\frac{\partial p}{\partial z}+\frac{\partial}{\partial x}\left(\mu_x\frac{\partial w}{\partial x}\right)+\frac{\partial}{\partial z}\left(\mu_z\frac{\partial w}{\partial z}\right) \tag{3}$$

Where u and w are the velocities in the x and z directions, respectively, ρ is water density, p is pressure, g is gravity acceleration, μ_x is horizontal eddy viscosity, μ_z is vertical eddy viscosity.

The concentration of any constituent in water, which is characterized by transport equation in two-dimensions, is governed by general equation below :

$$\frac{\partial C}{\partial t}+\frac{\partial(uC)}{\partial x}+\frac{\partial(wC)}{\partial z}=\frac{\partial}{\partial x}\left(K_h\frac{\partial C}{\partial x}\right)+\frac{\partial}{\partial z}\left(K_v\frac{\partial C}{\partial z}\right)+S \tag{4}$$

in which C is the concentration of the constituent, K_h is horizontal turbulent diffusivity, K_v is vertical turbulent diffusivity, and S is external sources or sinks of the constituent.

Discretization

The continuity and the momentum equations

In order to numerically solve the velocity and pressure fields, the equations (1)–(3) above were discretized by the finite-volume method. The method involves integrating the continuity and momentum equations over a two-dimensional control volume on a staggered differential grid (Patankar, 1980), as shown in Fig. 1.

In the staggered grid, the calculated domain is divided into control volumes defined by the dashed lines. The pressure is stored at the nodes marked (•) – the intersection of two unbroken grid lines and indicated by the capital letters P, W, E, N and S. The u-velocity components is stored at the east and the west cell faces of the control volume and indicated by the lower case letters e and w. The w-velocity components are located at the north and south cell faces of the control volume, which are indicated by the lower case letters n and s. Δ

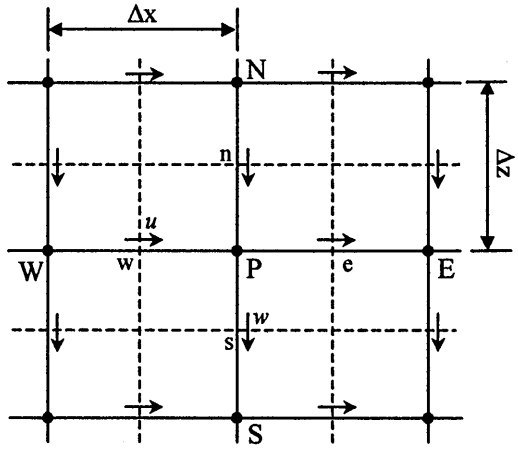

Fig. 1. Staggered grid describing a control volume with flow variables for two-dimensional situation.

x is the sub-interval of the calculated length. Δz is the sub-interval of the calculated depth.

After discretization, the discretized continuity equation becomes :

$$[(\rho u)_e-(\rho u)_w]\Delta z+[(\rho w)_s-(\rho w)_n]\Delta x=0 \tag{5}$$

and the discretized u-momentum equation becomes

$$a_e^{(u)}u_e=\sum a_{nb}^{(u)}u_{nb}+b^{(u)}+(P_P-P_E)\Delta z \tag{6}$$

with : $a_e^{(u)}=\dfrac{\rho_e^o\Delta x\Delta z}{\Delta t}+a_E^{(u)}+a_W^{(u)}+a_S^{(u)}+a_N^{(u)}$,

$$b^{(u)}=u_e^o\frac{\rho_e^o\Delta x\Delta z}{\Delta t}$$

and the discretized w-momentum equation can be written :

$$a_n^{(w)}w_n=\sum a_{nb}^{(w)}w_{nb}+b^{(w)}+(P_N-P_P)\Delta x \tag{7}$$

with : $a_n^{(w)}=\dfrac{\rho_n^o\Delta x\Delta z}{\Delta t}+a_E^{(w)}+a_W^{(w)}+a_S^{(w)}+a_N^{(w)}$,

$$b^{(w)}=-\rho_n g\Delta x\Delta z+\frac{w_n^o\rho_n^o\Delta x\Delta z}{\Delta t}$$

where : ρ_e^o, ρ_n^o, u_e^o and w_n^o refer to the known values at time t, while all other values are the unknown values at time $t+\Delta t$. The coefficients with superscripts (u) and (w) are the coefficients corresponding to u and w. $a_{nb}^{(u)}$, $a_{nb}^{(w)}$ refer to the neighbour coefficients $a_E^{(u)}$, $a_W^{(u)}$, $a_N^{(u)}$, $a_S^{(u)}$, $a_E^{(w)}$, $a_W^{(w)}$, $a_N^{(w)}$ and $a_S^{(w)}$, which account for the combined convection-diffusion influence at the control-volume faces of u-cell and w-cell, respectively. The values of these coefficients are obtained on the basis of the power-law scheme (Patankar, 1980). The velocity components u_{nb} and w_{nb} are those at the neighbouring nodes outside the control volume. P_E, P_W, P_N and P_S refer to the pressure at the east, the west, the north and

the south faces of the control volume, respectively.

The temperature equation

In principle, the equation (4) can be applied to any water quality variables. Within the conditions of this research, water temperature is chosen to illustrate the methodology. From the equation (4), we can write a transport equation for water temperature (T) as follows :

$$\frac{\partial T}{\partial t}+\frac{\partial(uT)}{\partial x}+\frac{\partial(wT)}{\partial z}=\frac{\partial}{\partial x}(K_h\frac{\partial T}{\partial x})$$

$$+\frac{\partial}{\partial z}(K_v\frac{\partial T}{\partial z})+\frac{1}{\rho C_p}\frac{\partial J_z}{\partial z} \quad (8)$$

where ρ is density of water, C_p is the specific heat of water, J_z is the solar radiation penetrating into water. The other symbols have been explained above.

To numerically solve for the water temperature in equation (8), it was also discretized by the finite–volume method. After the process of discretization, the discretized equation takes a form as follows :

$$a_P T_P=\sum a_{nb}T_{nb}+\frac{\rho\Delta x\Delta z T_P^o}{\Delta t}+\frac{[J_n-J_s]\Delta x}{\rho C_P} \quad (9)$$

where T_P^o is the known water temperature at the point P (the same as the point where pressure is stored in the staggered grid in Fig. 1) at time t. T_P is unknown water temperature at the point P at time $t+\Delta t$. J_n is the solar radiation influx of the control volume. J_s is the solar radiation outflux of the control volume. $a_P=\frac{\rho\Delta x\Delta z}{\Delta t}$ $+a_E+a_W+a_S+a_N \cdot a_{nb}$ refers to the neighbour coefficients a_E, a_W, a_S, a_N which account for the combined convection–diffusion influence at the control–volume faces of T–cell. The values of these coefficients are also obtained on the basis of the power–law scheme (Patankar, 1980). T_{nb} refers to unknown water temperature components at time $t+\Delta t$ at the neighbouring nodes outside the T_p–cell. The other symbols have been explained above.

Boundary Conditions

For calculation of velocities, boundary conditions at the bottom and the walls of lake are taken as the no–slip boundary condition ($u=w=0$). On the free water surface, w is set to zero, and u, which is set to 3% of wind speed at 10 m above water surface, is applied to the so–called reflection technique (Peyret and Taylor, 1983) in the calculation of the velocities.

For calculation of water temperature, the bottom and walls of lake are taken as adiabatic. The conditions on the free water surface are more complex because they involve heat exchange at the water surface between the atmosphere and the water in the lake. The heat fluxes through the water surface mainly include five parts (Shanahan, 1985), as shown in Fig. 2.

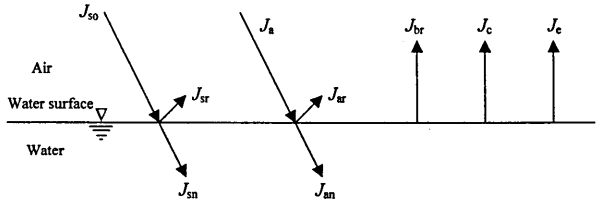

Fig. 2. Components of water surface heat exchange.

$$J=J_{sn}+J_{an}-(J_{br}+J_c+J_e) \quad (10)$$

Net solar shortwave radiation absorbed immediately at the surface (J_{sn})

$$J_{sn}=F_a J_{so}(1-\gamma) \quad (11)$$

where J_{so} is the incoming solar radiation (measured directly on site); γ is the water reflection coefficient (0.06); F_a is the fraction of the solar radiation that is absorbed immediately at the surface (0.65). The remaining the fraction of the solar radiation $(1-F_a)J_{so}$ is absorbed exponentially with depth as follows :

$$J_z=(1-F_a)J_{so}e^{-kez} \quad (12)$$

where z is the water depth and k_e is the extinction coefficient (0.5).

Net atmospheric longwave radiation (J_{an})

$$J_{an}=\delta(T_{air}+273)^4(A+0.031\sqrt{e_{air}})(1-R_L) \quad (13)$$

where δ is the Stefan–Boltzmann constant ($=5.67\times 10^{-8}$ W/(m^2 K^4)), T_{air} is the air temperature (°C), A is a coefficient (0.5 to 0.7), e_{air} is the air vapor pressure (mmHg), R_L is the reflection coefficient (≈ 0.03).

Longwave back radiation from the water (J_{br})

$$J_{br}=\delta\varepsilon_w(273+T_s)^4 \quad (14)$$

where δ is the Stefan–Boltzmann constant, T_s is water surface temperature, ε_w is emissivity (0.975).

Conduction (J_c)

$$J_c=0.47f(w)(T_s-T_a) \quad (15)$$

where T_s is water surface temperature, T_a is air temperature, $f(w)$ is the wind speed function, which is expressed $(9.2+0.46w^2)\times 7.6\times 10^{-4}$, w is wind speed.

Evaporation (J_e)

$$J_e=f(w)(e_s-e_a) \quad (16)$$

where $f(w)$ is the wind speed function $=(9.2+0.46w^2\times 7.6\times 10^{-4}$; w is wind speed, e_s is the saturation vapor pressure of air at the temperature of surface water (mmHg). It can be calculated as follows (Chapra, 1997) :

$$e_s=4.596e^{\frac{17.27T}{237.3+T}} \quad (17)$$

where T is air temperature

and e_a is the vapor pressure at 2 meters above the water surface (mmHg). The parameter e_a can be calculated as follows (Chapra, 1997):

$$e_a=\frac{e_s R_h}{100} \quad (18)$$

where R_h is relative humidity.

Numerical Algorithm

To solve equations (5)–(7), the SIMPLE algorithm (Patankar, 1980), which is essentially a guess-and-correct procedure for the calculation of pressure on the staggered grid introduced above, is applied. To initiate the SIMPLE calculation process, a pressure field p^* is guessed. The discretised momentum equations (6) and (7) are solved using the guessed pressure field to yield velocity components u^* and w^* as follows :

$$a_e^{(u)} u_e^* = \sum a_{nb}^{(u)} u_{nb}^* + b^{(u)} + (P_P^* - P_E^*)\,\Delta z \tag{19}$$

$$a_n^{(w)} w_n^* = \sum a_{nb}^{(w)} w_{nb}^* + b^{(w)} + (P_N^* - P_P^*)\,\Delta x \tag{20}$$

Defining the correction p' as the difference between the correct pressure field p and the guessed pressure field p^*, so that :

$$p = p^* + p' \tag{21}$$

Similarly defining the velocity correction u' and w' to relate the correct velocities u and w to the guessed velocities u^* and w^*:

$$u = u^* + u' \tag{22}$$

$$w = w^* + w' \tag{23}$$

By subtracting equations (19) and (20) from (6) and (7) respectively, it gives

$$a_e^{(u)}(u_e - u_e^*) = \sum a_{nb}^{(u)}(u_{nb} - u_{nb}^*) + [(P_P - P_P^*) - (P_E - P_E^*)]\,\Delta z \tag{24}$$

$$a_n^{(w)}(w_n - w_n^*) = \sum a_{nb}^{(w)}(w_{nb} - w_{nb}^*) + [(P_N - P_N^*) - (P_P - P_P^*)]\,\Delta x \tag{25}$$

Using the correction formulae (21)–(23), the equations (24) and (25) can be written as follows :

$$a_e^{(u)} u'_e = \sum a_{nb}^{(u)} u'_{nb} + (P'_P - P'_E)\,\Delta z \tag{26}$$

$$a_n^{(w)} w'_n = \sum a_{nb}^{(w)} w'_{nb} + (P'_N - P'_P)\,\Delta x \tag{27}$$

In the SIMPLE algorithm, the terms $\sum a_{nb}^{(u)} u'_{nb}$ and $\sum a_{nb}^{(w)} w'_{nb}$ are dropped to simplify equations (26) and (27) for velocity corrections. Therefore, we obtain :

$$u'_e = \frac{\Delta z}{a_e^{(u)}}(P'_P - P'_E) \tag{28}$$

$$w'_n = \frac{\Delta x}{a_n^{(w)}}(P'_N - P'_P) \tag{29}$$

Substituting equations (28) and (29) into (22) and (23) gives :

$$u_e = u_e^* + \frac{\Delta z}{a_e^{(u)}}(P'_P - P'_E) \tag{30}$$

$$w_n = w_n^* + \frac{\Delta x}{a_n^{(w)}}(P'_N - P'_P) \tag{31}$$

Similarly we have :

$$u_w = u_w^* + \frac{\Delta z}{a_w^{(u)}}(P'_W - P'_P) \tag{32}$$

$$w_s = w_s^* + \frac{\Delta x}{a_s^{(w)}}(P'_P - P'_S) \tag{33}$$

Substituting equations (30)–(33) into the discretised continuity equation (5), we draw the pressure-correction equation which plays an important part in the SIMPLE algorithm as follows :

$$a_P P'_P = a_E P'_E + a_W P'_W + a_N P'_N + a_S P'_S + [(\rho u^*)_w - (\rho u^*)_e]\,\Delta z + [(\rho w^*)_n - (\rho w^*)_s]\,\Delta x \tag{34}$$

where : $a_P = a_E + a_W + a_N + a_S$

$$a_E = \rho_e \frac{(\Delta z)^2}{a_e}\ ;\ a_W = \rho_W \frac{(\Delta z)^2}{a_w}\ ;$$

$$a_N = \rho_N \frac{(\Delta x)^2}{a_n}\ ;\ a_S = \rho_S \frac{(\Delta x)^2}{a_s}\ ;$$

The procedure of the SIMPLE algorithm, which is applied at each time step, is summarized in a flow chart as shown in Fig. 3 below.

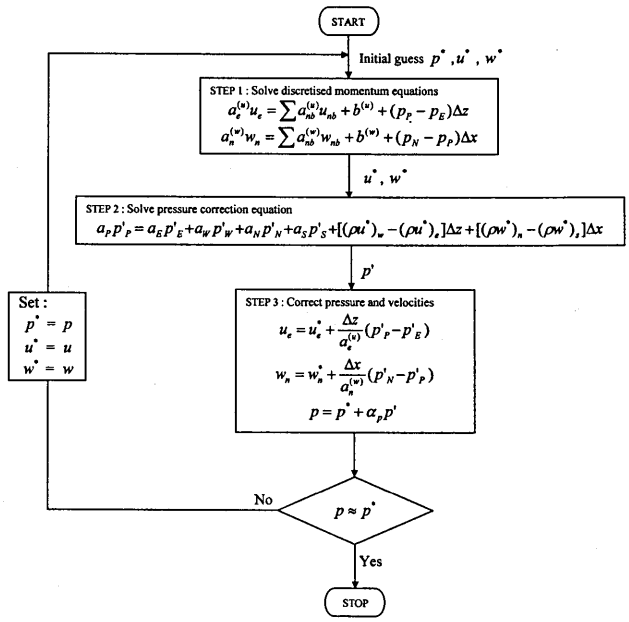

Fig. 3. Flow chart of the SIMPLE algorithm.

In Fig. 3, α_p is the pressure under-relaxation factor, the other symbols have already been explained above.

The SIMPLE algorithm is extended to transient calculations to cover the desired time period. A flow chart for the calculation of unsteady-state flows will be shown in Fig. 4.

In Fig. 4, ϕ represents water quality variables (water temperature, dissolved oxygen...), t is time, Δt is the calculated time step, t_{max} is the desired time period.

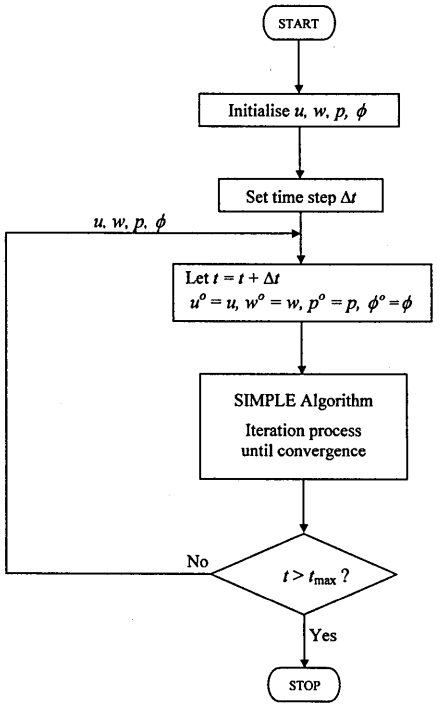

Fig. 4. Flow chart for unsteady flow calculation with application of the SIMPLE algorithm.

Other symbols were already explained above.

In performing the SIMPLE algorithm to solve velocities and calculation of water temperature, the TDMA (Tri-Diagonal Matrix Algorithm) or Thomas' algorithm, which has become almost standard for the treatment of tridiagonal systems of equations (Anderson, 1995), is employed by line-by-line method.

To solve a general two-dimensional discretised equation with a form such as :

$$a_P \phi_P = a_W \phi_W + a_E \phi_E + a_S \phi_S + a_N \phi_N + b \qquad (35)$$

the equation can be re-arranged in the form :

$$-a_S \phi_S + a_P \phi_P - a_N \phi_N = a_W \phi_W + a_E \phi_E + b \qquad (36)$$

Considering the discretized equations for the grid points along a chosen line (shown by •), we can see that they contain the variables at the grid points (shown by □) along the two neighboring lines (ϕ_W and ϕ_E). If the right hand side of the equation (36) is assumed to be temporarily known, the equations along the chosen line (shown by •) would look like one-dimensional equations and could be solved by the TDMA. Subsequently the calculation is moved to the next line. If we sweep from west to east, the values of ϕ_W to the west of point P are known from the calculation performed on the previous line. Values of ϕ_E to its east, however, are unknown, so the solution process must be iterative. The line-by-line calculation procedure is repeated several times until a converged solution is obtained. The method is illustrated in Fig. 5. (Versteeg and Malalasekera, 1995).

Where the points (•) at which the values are calculated, the points (□) are considered to be temporarily known,

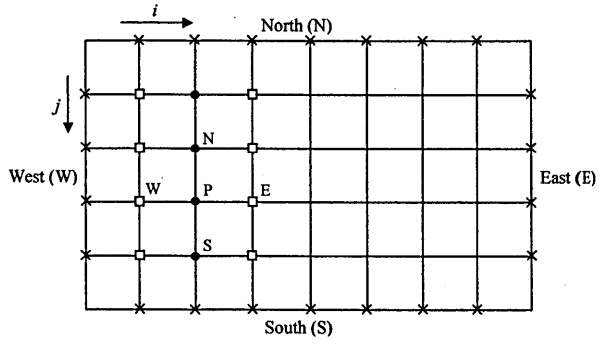

Fig. 5. Illlustration of the line-by-line method.

and the points (×) are known boundary values.

Data requirement for the model

To calculate the velocities and simulate water temperature, three kinds of data must be collected as follows.

+ *Meteorological data of the study area* : The first type of data necessary to collect are meteorological data in the study area. Sensors for measuring wind direction, wind velocity, air temperature, and relative humidity are set up, and these parameters are measured every 2 minutes.

+ *Water temperature data* : Along the depth of the lake, the water is divided into layers and the water temperature is measured at each layer. The data are measured every hour during a daily period of 24 hours for calibrating the model. The measurement is made on site by using the W-23XD multi probe (Horiba, Ltd., 2001).

+ *The lake size data* : In addition to water temperature and meteorological data, the data on lake size such as the average depth of the lake (H), the average length of the lake (L) must be collected.

Calibration process

Calibration is the process through which one or more parameter inputs of the model are adjusted so that the model has its best fit with the observed data set. In

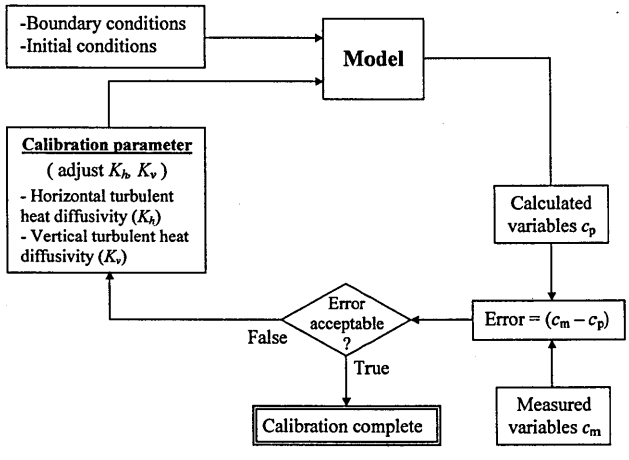

Fig. 6. The process of model calibration.

this model, the parameters chosen to be calibrated are horizontal turbulent heat diffusivity (K_h) and vertical turbulent heat diffusivity (K_v).

By the trial–by–error method, we can calibrate the model by adjusting the horizontal turbulent heat diffusivity (K_h) and the vertical turbulent heat diffusivity (K_v) until the results of the simulation have their best fit with the observed data sets. The process of calibration is implemented as illustrated in Fig. 6.

In Fig. 6, c_p, c_m represent calculated and measured water quality variables (water temperature, dissolved oxygen...). In this research, water temperature is taken to calibrate.

RESULTS AND DISCUSSION

Model calibration

To verify the model, Tabiishidani lake, which is located in Sasaguri – Fukuoka prefecture in Japan, was chosen. The lake has an average depth of 2.2 m. The length is about 80 m. In general, the volume of inflow and outflow is zero; that is, there are no changes in water level.

In a cross–section of the lake, the length is sub–divided into intervals of 2 m, the depth is sub–divided into intervals of 0.2 m to create control volumes with the size (2 m × 0.2 m). The calculated domain is arranged on a staggered grid as illustrated in Fig. 1 above. The calculated time step (Δt) is set to 1800(s). The calculation covers a time period of 24–hour day.

The temperature distribution in the lake was measured at 15:00 on June 26, 2003 and at 20:00 on September 26, 2003, which are taken as the initial conditions of temperature (see Figs. 7 & 8).

Meteorological data such as relative humidity, solar radiation, air temperature, and wind speed were also measured on the same day that water temperature was measured. The measurement of meteorological data covers a 24–hour day.

Numerical simulations were performed and the results were compared with the observed data. Figs. 9 & 10 show the results of water temperature simulations against the observed data on June 26, 2003 and September 26, 2003, respectively. From the Figs. 9 & 10

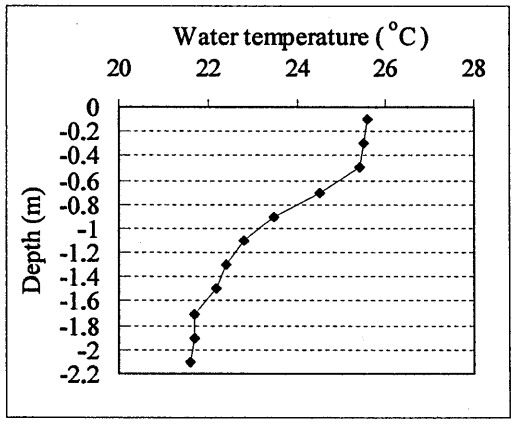

Fig. 7. Water temperature distribution in the lake was measured at 15:00 on 06/ 26, 2003.

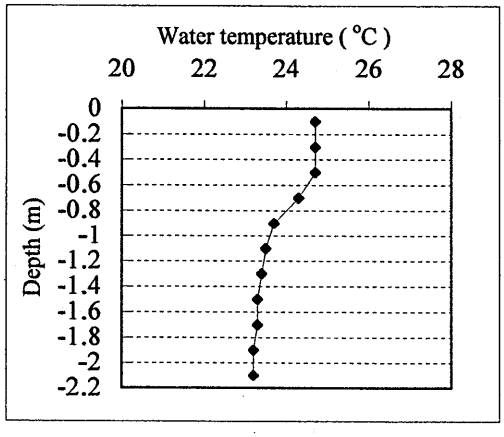

Fig. 8. Water temperature distribution in the lake was measured at 20:00 on 09/ 26, 2003.

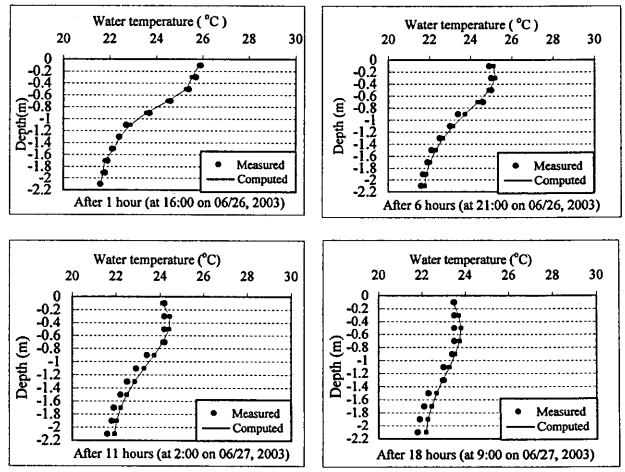

Fig. 9. The results of water temperature simulations against the observed data on June 26 & 27, 2003.

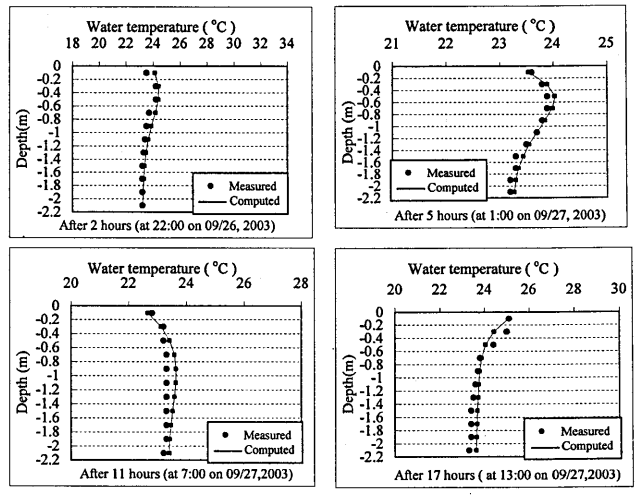

Fig. 10. The results of water temperature simulations against the observed data on September 26 & 27, 2003.

we can see that the results of simulations have a good fit with the observed data sets. Therefore, the model can be reliable to simulate water temperature under different meteorological patterns and different patterns of initial temperature.

Application

After calibration, the model is applied to simulate water temperature under assumed meteorological patterns and an assumed initial temperature distribution.

Case 1 : Figs. 11.1 & 11.2 describe a meteorological pattern representing a typical day in winter.

Assuming that on that day, water temperature distribution along the depth of the lake is homogeneous and equal to 6.5 °C at 7:00 am. This distribution is used as the initial condition of water temperature for the model. From this initial condition along with the assumed meteorological pattern described in Figs. 11.1 & 11.2, the model has simulated the change in water temperature distribution along the depth of the lake over a 24–hour day.

The results of the simulation are shown in Fig. 12.

From Fig. 12 we can see that the change in water temperature distribution in the lake can be divided into two

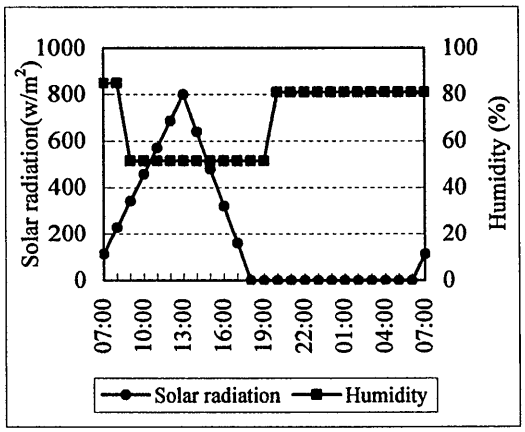

Fig. 11.1. Solar radiation and humidity patterns representing a typical day in winter.

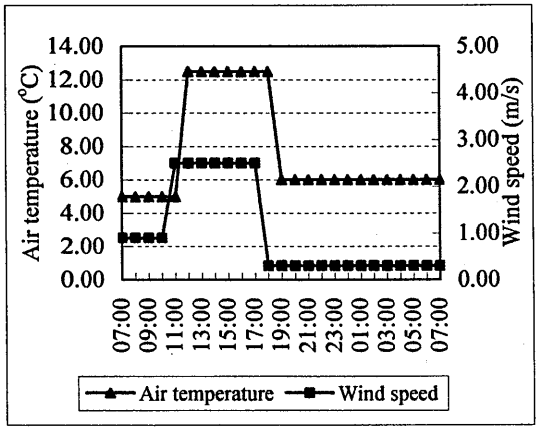

Fig. 11.2. Air temperature and wind speed patterns representing a typical day in winter.

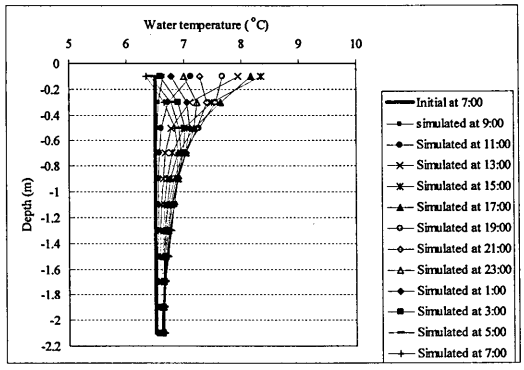

Fig. 12. The results of simulation on water temperature distribution along the depth of the lake over a 24–hour day in winter.

main periods as follows :

a) The first period from 7:00 am to 15:00 pm : During this period the water temperature distribution gradually changes from a homogeneous state to a stratification of temperature. The thermal stratification gradually developes and reaches its maximum value at 15:00 pm. At 15:00 pm, the temperature gradient between the upper layer and the bottom layer is at its maximum. The reason for this phenomenon is that from 7:00 am to 13:00 pm solar radiation and air temperature increase and get their peak at 13:00 pm. As a result, during this period, the water is heated and the water temperature gradually increases. Due to the fact that the upper layer absorbs almost of solar radiation, the water temperature in the upper layer is highest while that in the lower layers decreases less and less as the depth is deeper because solar radiation is absorbed decreasingly with depth according to an exponential law. It can be seen that solar radiation reaches a peak at 13:00 pm while the thermal stratification gets its maximum value, and the water temperature in the upper layer is highest at 15:00 pm. That is because it takes time to transfer the heat energy from solar radiation into the water. This period can be called *the heating period* of the lake.

b) The second period from 15:00 pm to 7:00 am of next day : It can be seen from the Fig. 12 that after the thermal stratification gets its maximum value at 15:00 pm, the water temperature in the upper layers decreases gradually, and temperature gradient between the upper layer and the bottom layer also decreases gradually. It is easily seen that the water temperature distribution tends to return to the initial state (homogeneous state), and the water temperature in the upper layer returns to a value nearly equal to the initial value at 7:00 am the next day. This change can be explained that during this period, solar radiation decreases gradully and becomes extinct at about 19:00 pm. Therefore, the energy to heat water in the lake also decreases. As a result, it leads to a gradual decrease in water temperature. Besides, during this period, at night the air

temperature also falls to a value lower than the water temperature, causing the loss of energy from water to air. This phenomenon also contributes to the decrease in water temperature during this period. This period can be called *the cooling period* of the lake.

From Fig. 12 we can see that the amplitude of the change in water temperature is largest in the upper layer. This amplitude becomes smaller and smaller in the lower layers.

It can be seen that the significant change in water temperature takes place mainly in the layers in the top one–third of the lake, while the change in water temperature in the layers in the bottom two–thirds of the lake is unremarkable. This can be explained that due to weak wind on that day, the effect of circulation in the lake by mixing the upper layers into lower layers is small. That's why water temperature in the lower layers changes unremarkably while that in the upper layers is affected greatly by solar radiation, and thus changes significantly.

Case 2 : Figures 13.1 & 13.2 describe a meteorological pattern representing a typical day in summer.

This pattern of meteorology and water temperature

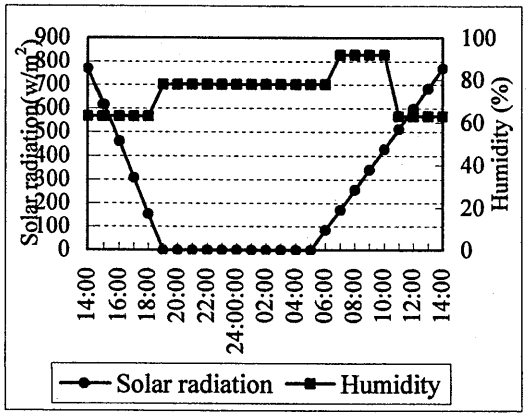

Fig. 13.1. Solar radiation and humidity patterns representing a typical day in summer.

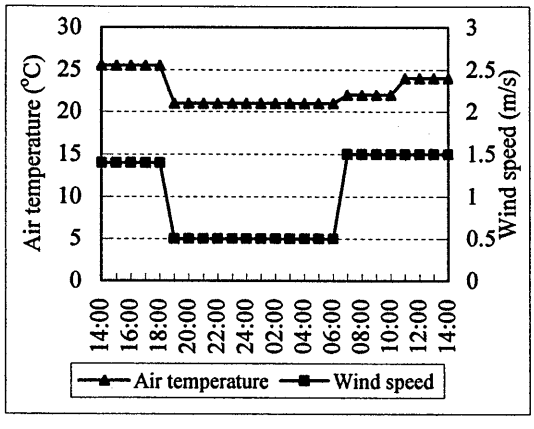

Fig. 13.2. Air temperature and wind speed patterns representing a typical day in summer.

distribution is assumed, as illustrated by the bold line in Fig. 14. This set of water temperature represents the state of thermal stratification in the lake at the time (14:00 pm) when solar radiation and air temperature reache a peak on a day in summer. This condition is used as the initial condition of water temperature for the model to simulate the change in temperature distribution over a 24–hour day. The results of the simulation

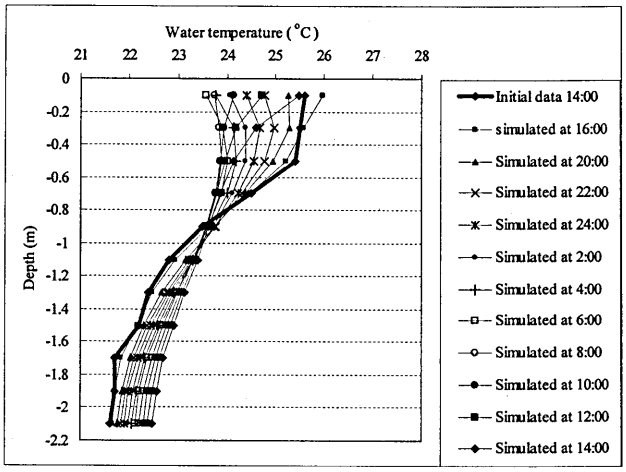

Fig. 14. The results of simulation on water temperature distribution along the depth of the lake over a 24–hour day in summer.

are shown in Fig. 14 below.

It can be seen from Fig. 14 that the change in water temperature distribution can be also divided into two main periods as follows :

a) The first period from 14:00 pm to 6:am of next day : During this period, water temperature in the top one–third of the lake tends to decrease gradually while in the lower layers water temperature increases little by little. At the initial time (14:00 pm), water temperature gradient between the upper layer and the bottom layer is largest. However, at the end of this period this gradient becomes smallest. This phenomenon can be explained that during this period solar radiation decreases gradually, and it is extinct at night. Therefore, the energy to heat water also decreases. As a results, it leads to a water temperature decrease in the upper layers. In addition to that, at night air temperature falls to a value lower than water temperature, causing the heat loss from water to air. This contributes to the decrease in water temperature in the upper layers. Also, the phenomenon of circulation in the lake contributes to the gradual decrease in water temperature gradient between the upper layer and the bottom layer. Wind acting on the water surface causes a flow called the wind–induced flow in the lake. This flow works to mix the warmer waters in the upper layers into the cooler waters in the lower layers. The stronger wind blows the more effective the mixing is. This mixing, which is called the circulation of lakes, helps to lessen water temperature gradient between the upper layers and the

lower layers.

b) The second period from 6:00 am to 14:00 pm : During this period water temperature in the upper layers increases gradually because the increasing solar radiation heats the water in the lake. Due to circulation of the lake, water temperature in the lower layers also increases little by little during this period. However, the water temperature gradient between the upper layer and the bottom layer increases gradually and get its maximum value at 14:00 pm.

CONCLUSIONS

From the results presented above, some conclusions can be drawn as follows :

- In general, the results of the simulation have good agreement with the observed data. Therefore, the model is reliable to simulate water temperature distribution in lakes under different meteorological patterns.
- During a daily cycle, thermal regime in lakes undergoes two main periods namely *the heating period* and *the cooling period*. The heating period usually takes place during the period when solar radiation is present to heat water in lakes and causes the thermal stratification to reach its maximum value. The cooling period usually takes place during the period when solar radiation falls sharply and during the night–time when air temperature decreases significantly.
- From the results of the simulation above we can see that the amplitude of the change in water temperature is largest in the upper layer. It becomes less and less in the lower layers. In other word, water temperature in the upper layers is influenced greatly by the climate conditions and varies significantly. In contrast, the change in water temperature belonging to the bottom layers is unremarkable except when the circulation of lakes takes place significantly.
- The circulation induced by wind can play a part in the change in water temperature distribution of lakes by narrowing water temperature gradient between upper layers and bottom layers through mixing waters in upper layers into lower layers.
- The model is based on some simplifying assumptions. The key assumptions of the model are :
  + The lake is assumed to be well–mixed laterally. In other word, the model is calculated on the basis of two–dimension.
  + The density of water is homogeneous vertically

REFERENCES

Anderson, J. D 1995 *Computational fluid dynamics.* McGraw–Hill, Inc., New York, pp. 150–442

Chapra, S. C 1997 *Surface water–quality modeling.* McGraw–Hill, New York, pp. 26–650

Cole, T. M and E. M. Buchak 1995 CE–QUAL–W2: A two–dimensional, laterally averaged, hydrodynamic and water quality model, Version 2.0. *Users Manual, Instruction Report EL–95–1.* U.S. Army Engineer Waterways Experiment Station, Vicksburg, MS, pp. 19–25

Imberger, J. and J. C. Patterson 1981 A dynamic reservoir simulation model–DYRESM. *In* "Transport Models for Inland and Coastal Waters", ed. by H. B. Fischer, Academic Press, New York, pp. 310–361

Mori, K., S. Shikasho and K. Hiramatsu 2001 Wind–induced flow in a closed–water area with discrete wind shear. *Fisheries Engineering* **37**(3): 195–201

Nyhoff, L. and S. Leestma 1997 *Fortran 90 for Engineer and Scientists.* Prentice Hall, America, pp. 30–46

Nyhoff, L. And S. Leestma 1999 *Introduction to Fortran 90.* Prentice Hall, America, pp. 15–196

Patankar, S. V 1980 *Numerical heat transfer and fluid flow.* McGraw–Hill, New York, pp. 41–143

Peyret, R. and T. D Taylor 1983 *Computational methods for fluid flow.* Springer–Verlag, New York Heidelberg Berlin, pp. 150–153

Rounds, S. A and T. M. Wood 2001 Modeling Water Quality in the Tualatin River, Oregon, 1991–1997: U.S. Geological Survey Water–Resources investigations Report 01–4041, pp. 6–11

Shanahan, P 1985 Water Temperature Modeling: A Practice Guide. *In* "Proceedings of Stormwater and Water Quality Model Users Group Meeting, April 12–13, 1984". EPA–600/9–85–003, pp. 1–13

Versteeg, H. K. and W. Malalasekera 1995 *An introduction to computational fluid dynamics.* Longman House, Burnt Mill, Harlow, pp. 135–159